

Piotr WALKER
Błażej DOROSZUK
Robert KRÓL

ANALYSIS OF ORE FLOW THROUGH LONGITUDINAL BELT CONVEYOR TRANSFER POINT

BADANIA SYMULACYJNE PRZESYPY WZDŁUŻNEGO PRZENOŚNIKA TAŚMOWEGO

A transfer point is an element of a belt conveyor prone to increased energy losses and to the risk of failure. It is also a location in which the receiving belt is particularly susceptible to damage. Except failure-free operation, a transfer point should offer minimal belt resistances to motion by ensuring that the transported material is placed centrally on the receiving belt, both spillage of the material and blockages are prevented, the process of particle defragmentation is limited, and also that noise and dust emissions to the environment are reduced. Ensuring that the above requirements are met requires inter alia the use of advanced simulation tests. The article analyzes the flow of ore particles stream through a longitudinal transfer point used in an underground copper ore mine. Discrete Element Method was used to identify the phenomena which occur while transferring ore onto the receiving conveyor. The research allowed key variables affecting the transfer point performance to be identified. It also resulted in a proposal of actions which can improve the performance of the transfer point and which are focused on saving energy and on minimizing the damage and wear of the receiving belt.

Keywords: transfer point, Discrete Element Method, conveyor belt, abrasive wear, cumulative contact energy.

Przesyp jest miejscem przenośnika taśmowego, w którym pojawia się ryzyko wystąpienia awarii, występują straty energii oraz może dochodzić do uszkodzenia taśmy odbierającej urobek. Poza bezawaryjnym funkcjonowaniem przesyp powinien dla zminimalizowania oporów ruchu taśmy zapewnić także centralne podawanie urobku, zapobiegać rozsypywaniu się transportowanego materiału, nie dopuszczać do powstawania zatorów, ograniczać proces defragmentacji urobku, a także minimalizować emisję hałasu oraz pyłów do otoczenia. Zapewnienie stawianych wymagań wiąże się z koniecznością stosowania m.in. zaawansowanych badań symulacyjnych. W artykule przeprowadzono analizę przepływu strugi urobku przez wybrany przesyp wzdłużny, stosowany w podziemnej kopalni rud miedzi. Przy użyciu metody elementów dyskretnych DEM dokonano oceny zjawisk zachodzących podczas przesywania rudy na przenośnik odbierający, wskazano kluczowe zmienne opisujące jego pracę, a także zaproponowano działania udoskonalające pracę przesypu, zorientowane na zwiększenia jego energooszczędności oraz zmniejszenia negatywnego oddziaływania transportowanego osiwa na taśmę przenośnika odbierającego.

Słowa kluczowe: punkt przesyowy, Metoda Elementów Dyskretnych, taśma przenośnikowa, zużycie ściernie, skumulowana energia kontaktowa.

1. Introduction

The function of the transfer point is to pass the transported material from the feeding conveyor to the receiving conveyor in such a manner as to prevent the material from being blocked [19]. In the case when a transfer point is badly designed, the transportation process may be interrupted, subjecting the mining company to considerable financial losses [12]. According to [10], downtime of the main belt conveyor in a copper mine in Chile, which produces 100,000 metric tons of ore per day, may lead to as much as \$250,000 loss per hour. Except failure-free operation, a transfer point should offer minimal belt resistances to motion by ensuring that the transported material is placed centrally on the receiving belt, both spillage of the material and blockages are prevented, the process of particle defragmentation is limited, and also that noise and dust emissions to the environment are reduced [17].

Three transfer point design methods are currently used: analytical, simulational and experimental. The first analytical investigation of the

trajectory of the material flowing through a transfer point was offered by C.E.M.A [1] in the 1960s. In 1988, Korzeń [20] presented an improved method for calculating the required hood curve (in hood and spoon transfer) and the particle flight path which allows calculations to be performed for both cohesive and non-cohesive materials. This topic was further researched by Roberts in 2003 [23]. In his calculations, Roberts allowed for the friction between the particles and the elements of the transfer point, as well as for particle humidity. Over the following years, with increasing computational power available, transfer points started to be designed with the use of simulations based on Discrete Element Method (DEM), which consist in preparing a three-dimensional model of the investigated transfer point and in performing subsequent multi-variant analyses of how the design and operational parameters influence the transport of the material. In DEM simulations, forces acting on individual ore particles are determined at very short time intervals. In the first step, the algorithm identifies the total forces acting on the particles, and subsequently uses Newton's second law to find the acceleration and displacement for each of the

(*) Tekst artykułu w polskiej wersji językowej dostępny w elektronicznym wydaniu kwartalnika na stronie www.ein.org.pl

particles [18]. The two calculations are performed for one time step, and the algorithm proceeds to perform calculations for the next time step, using the data obtained in the previous step [14]. In order to simulate interactions between the particles, contact models are used.

Experimental, laboratory tests of transfer points are performed on specially adapted test stands, which employ high-speed cameras to identify the flow of material. The cameras allow an analysis of several tens to several hundreds of frames per second. Publication [11] describes an analysis of ore-flow through a transfer point, performed with the use of both analytical and simulation methods, and compares the effects with the experiment results. The research demonstrates that simulation methods have advantage over other methods. Publication [15], on the other hand, offers a comparative analysis of the analytical method proposed by Roberts [23] and of the DEM method, and indicates a high correlation between the results, while pointing to the limitations of the analytical methods.

The operation of the transfer points is related to the occurrence of concentrated resistances in the location where the material is fed [8]. Preliminary analyses performed for the KWB Bełchatów lignite mine suggest that these resistances may account for approximately 5% of the power loss on the conveyor [7]. The resistances occur when the material fed to the receiving conveyor has lower velocity tangential to the belt movement direction than the velocity of the belt itself, which indicates that the velocity of the material must be increased. Another component of the resistances is the friction of the material against the side skirts. Side skirts are used in the transfer point and installed over the belt of the receiving conveyor. They are located in the zone where the stream of material is formed and their function is to prevent individual grains from spilling outside the belt and to form the material into a shape appropriate for further transportation. As the material dropped on the receiving belt is typically characterized by turbulent movement, it should be stabilized before it leaves the skirts [3]. Additionally, during its flight, the transported material significantly increases its normal component of the velocity vector with respect to the conveyor plane. Therefore, when dropped on the belt, it may cause its damage and also negatively influence the condition of the feeding idler sets [21].

2. Simulation preparation

2.1. Calibration process

The effectiveness of the DEM simulations largely depends on the input parameters describing the simulated bulk material [2, 16]. The parameters used as the preliminary source of data for the calibration process of the investigated copper ore were obtained as part of own research [6]. The volumetric density was averaged on the basis of several samples, and the restitution coefficient was determined for steel, rubber and 3 types of rock present in the deposit. The ore-ore friction coefficient was determined with the use of a direct shear apparatus, and the ore-steel and ore-rubber coefficients were found with the use of an inclined

plane. The rolling friction coefficient was assumed at 0.01, and other parameters were assumed on the basis of detailed literature studies, described in [6].

The test stand used in the experiment was similar in design to the stand described in [22]. It is a cubical box with a container holding the tested material in its upper part. The material slides on a plane which has variable inclination angle and which is located under the container. Upon releasing the lock, the sample stored in the container is allowed to leave it in the form of a stream of material which hits the plane and slides on it, eventually forming a fragment of a pile in the corner of the box. For the purpose of the tests, the device described in [22] was modified in such a manner that the material of the sliding plane could be modified. As a result, contact parameters were obtained for both steel and the carrying cover of the conveyor belt. In order to enable detailed observation of the behavior of the tested ma-

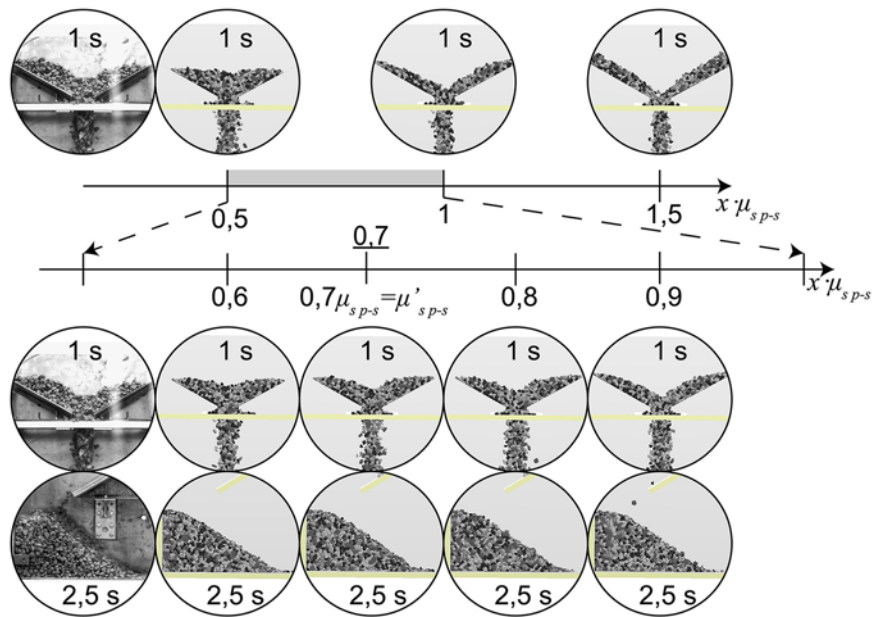


Fig. 1. Calibration step for particle-steel (p-s) coefficient of static friction (μ_s) – comparison of the characteristic parts of the simulation after 1 and 2.5 seconds for different multipliers (x) of friction coefficient

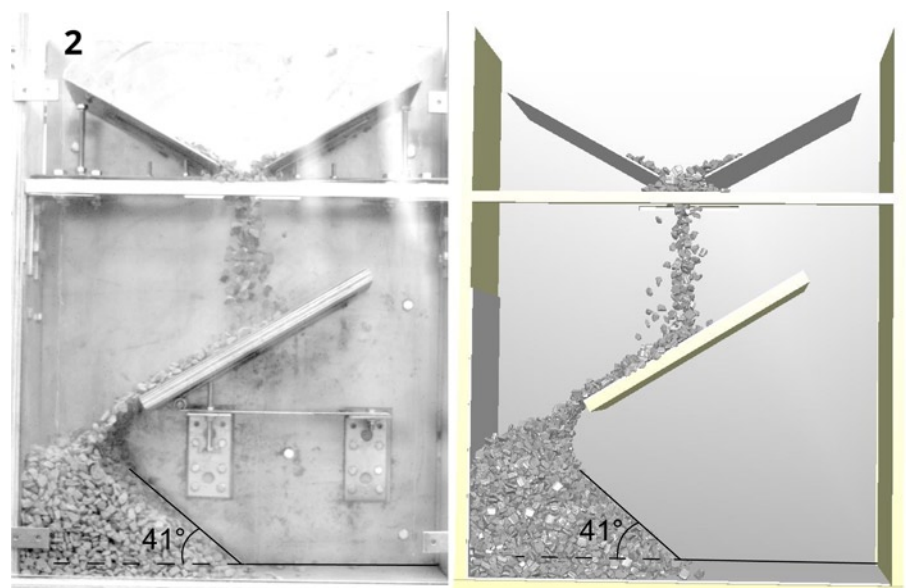


Fig. 2. On the left: a frame from the recorded experiment; on the right: the corresponding moment of the simulation

material, the experiments were recorded with the use of Phantom Miro 120 high-speed camera, at 600 frames per second.

A number of simulations were performed, with each of the parameters modified in succession. The simulations were subsequently compared with the recorded experiments (Fig. 1). In the first step, the calibration process included the ore-ore contact parameters, and in the second stage – the ore-rubber parameters. As a result, a calibrated model was obtained for copper ore, which reflected the behavior of the actual material (Fig. 2) [5].

2.2. Preparation of the model

In the modeling process, the conveyor belt trough was filled with particles generated by the EDEM application. Their behavior was simulated with the use of the discrete element method and with allowance for the calibrated material parameters of the mined copper ore.

Fig. 3 shows a simplified 3D model of the actual longitudinal transfer point operated in the mine. The transfer point comprised an adequately shaped upper (feeding) belt, lower (receiving) belt, feeding conveyor drum and side skirts. The geometry was modeled in the form of meshed surfaces with zero thickness. Only those surfaces were modeled which can be contacted directly by the transported material. This fact is due to the complexity of the calculation algorithm (and especially the detection of potential contacts between the material and the skirting elements), whose efficiency is also affected by the geometrical complexity of the model. The resulting geometry simulates the system to a satisfactory degree and is sufficient to perform DEM analyses.

In order to fully represent the grain size distribution, the SplitDesktop application was used to perform analyses on the basis of the collected photographic documentation of the material present on the top run of the feeding conveyor [24]. Only particles greater than 50 mm in diameter were modeled in the simulation, as the finer fraction would significantly increase the simulation preparation time, while its absence does not affect the results. Particles finer than 50 mm were cumulated and added to the finest generated fraction. In the simulation, the total assumed stream of the material mass at maximum capacity of the B1200 conveyor was 2072 Mg/h.

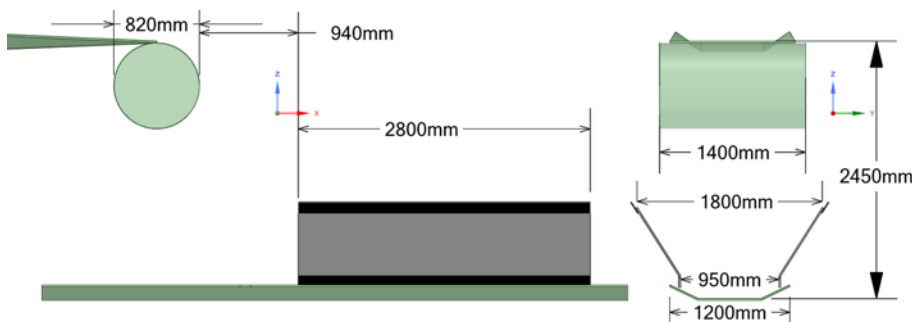


Fig. 3. Simplified 3D model of the analyzed transfer point used for the needs of the DEM simulation

3. Simulation

The criterion for the evaluation of the transfer point operation was based on component velocities of the material at the moment of collision with the belt. Known component velocities allow calculating abrasive wear of the belt at the location where the material accel-

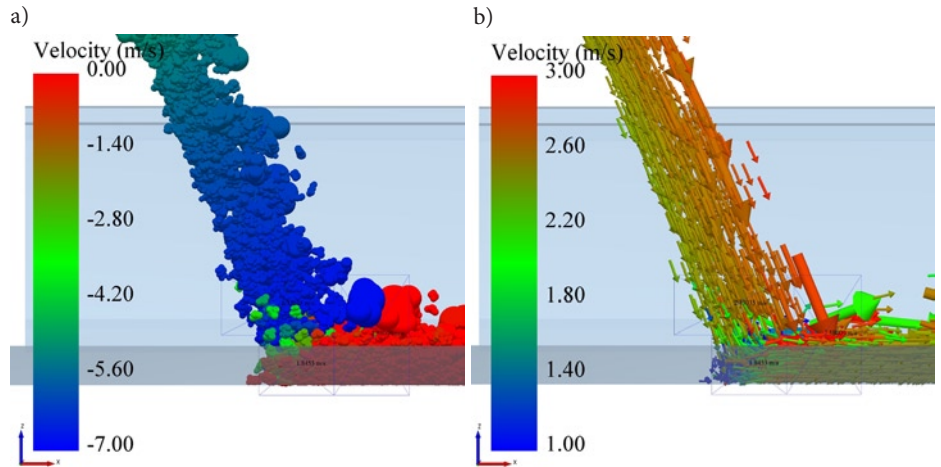


Fig. 4. View of the collision between the material and the belt during a DEM simulation: a) normal velocity of particles (recorded along the Z axis), b) tangential velocity of particles (along the X axis)

erates. Material velocity tangential to the belt surface influences the energy-consumption of the transfer point and its concentrated resistances. When this velocity is lower than the velocity of the conveyor belt, losses occur [8, 9, 21]. However, velocity normal to the belt surface causes impact-related destruction of the carrying cover and of the feeding idler sets.

The analyzed design of the transfer point is a commonly used solution, in which the material is transferred directly from the belt of the feeding conveyor onto the belt of the receiving conveyor. Simulations demonstrated that at the moment of collision with the receiving belt, the stream of material has a normal velocity of approximately 6.3 m/s, which is further reduced so that in effect the entire energy of the falling material is received by the belt (Fig. 4a). In addition, virtual velocity sensors were added for individual particles in order to allow defining mean normal and tangential velocities of material particles during and after the impact.

In Fig. 4b, the vectors serve to present the analysis of particle behavior along axis X. Prior to the impact, the particles moved with a static velocity of approximately 2.37 m/s. At the moment of contact with the belt, the particles lost their velocity to 1.73 m/s and were subsequently accelerated, by the friction forces acting between the belt and the material, to the rated velocity of the belt (2.5 m/s). In order for the material to be accelerated, the friction force between the material

and the belt must be greater than both the lift resistances of the material due to the inclination angle of the conveyor and the friction resistances of the material due to the side skirts [8]. This phenomenon accounts for the additional resistance to motion generated at the feed point.

The EDEM application was used to calculate the values of the energy received by the top run in the receiving conveyor over a 30-second period of its operation at rated capacity. For this purpose, the belt was divided into segments consisting of right triangles having sides 10 cm in length. Subsequently, the cumulated value of tangential and normal energy was calculated. The result served as a basis for identifying those belt fragments of the receiving conveyor which

are most prone to wear. The simulations demonstrated that the greatest amount of energy is received by the middle fragment of the belt and by the side fragments. Less energy is received in the deflection zone on the idler set (Fig. 5).

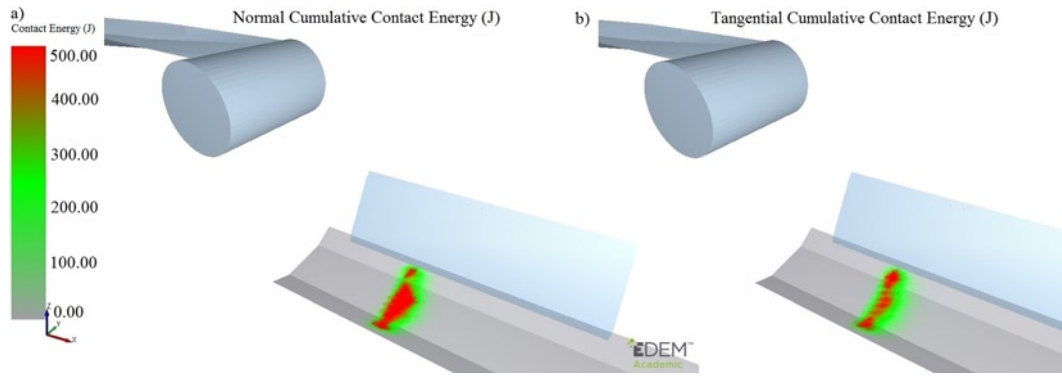


Fig. 5. Cumulative normal (a) and tangential (b) contact energy values determined in the EDEM software during the contact between the receiving conveyor belt and the material in the variant before modification

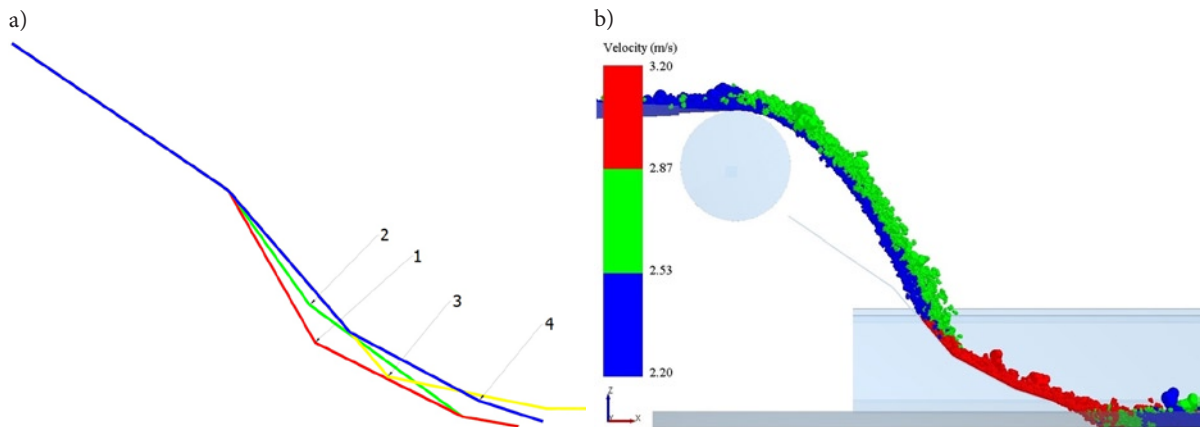


Fig. 6. Analyzed variants of the chute considered during the simulation tests (a) and the behavior of the material during the flows through chute No. 4 (b)

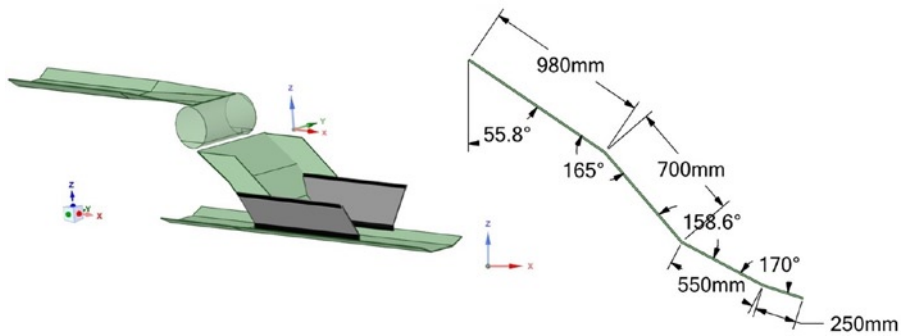


Fig. 7. Proposed design solution for longitudinal transfer chute

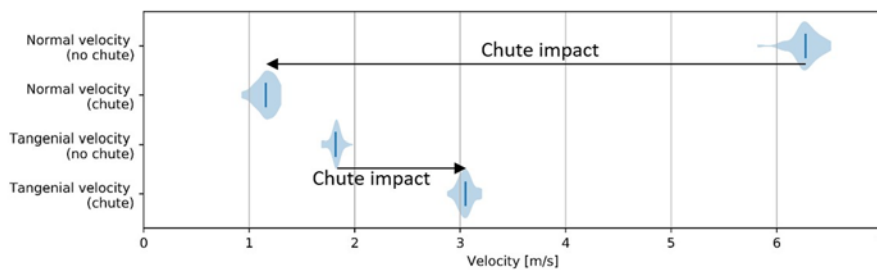


Fig. 8. Violin plot of tangential and normal velocity values recorded at the moment of the collision between the material and the belt for the tested variants of the longitudinal transfer point with indicated average velocity values

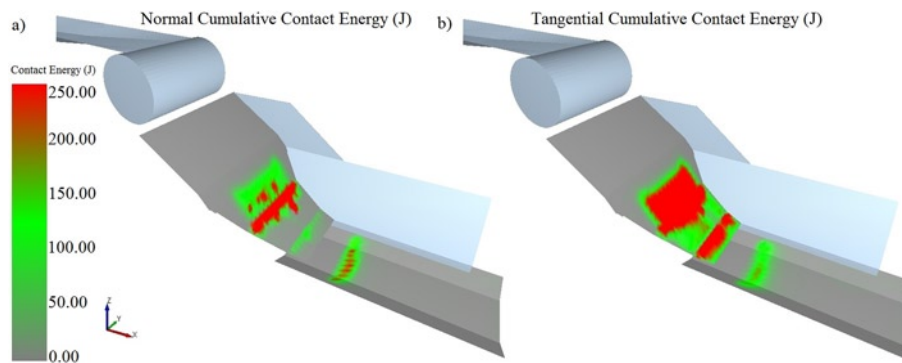


Fig. 9. Cumulated values of normal (a) and tangential energy (b) resulting from the contact of the transported material with the chute and with the receiving conveyor belt in the modified variant

As the analyzed transfer point is operated in a system of belt conveyors working at a constant speed of 2.5 m/s, the proposed optimizing solution was a chute. A chute appropriately adjusted to the discharge trajectory at the transfer point should reduce the value of the material component velocity normal to the belt and adjust its component tangential to the velocity of the receiving conveyor belt [9, 21].

The simulations were performed on four selected variants of the chute slope, with different numbers of plates and with their various inclination angles with respect to the vertical (Fig. 6a). The design differences in the tested solutions resulted from successive simulations of material behavior, during which the sensors available in the EDEM application were used to analyze the velocity components at the moment of material collision with the belt [13].

Fig. 6b shows changes of the tangential velocities of the material particles during the simulations for chute No. 4. Upon the collision with the receiving plate, the material was observed to increase its tangential velocity, which was then partly reduced due to friction against the lower section of the chute. As a result, the material acquired a velocity similar to the velocity of the receiving belt. Fig. 7 shows the geometric dimensions of the chute which provided the best optimization results.

Analogically to the analyses performed for the basic version, in the case of the accepted solution, both tangential and normal velocity components were also calculated for the material at the moment of collision with the belt. Fig. 8 shows a comparison of the obtained values. In the variant of the transfer point with a chute, the tangential velocity variable in time oscillates in the range from 2.8 m/s to 3.2 m/s, with mean velocity at approximately 3 m/s. This fact implies that the material is fed faster than the belt moves, and at the same time this value is sufficiently small not to cause the material to be spilled outside the transfer point. With the modernized version of the transfer point, the tangential velocity of material particles was increased by 1.2 m/s on average. Meanwhile, the calculated mean normal velocity of material particles in this variant is as much as 6-fold smaller and is approximately 1.15 m/s. This decrease allows a significant reduction of the destructive influence of the potential energy of the material masses falling on the conveyor belt and on the supporting idler sets.

Values of accumulated contact energy were used in order to identify the chute sections most susceptible to abrasive wear (Fig. 9). The sections of the chute most prone to damage due to normal and tangential forces have been indicated in red. Failure-free operation of the chute can be ensured by installing additional reinforcements in selected chute fragments (for example by using an appropriate construction material), and by frequently controlling their technical condition.

A comparison of the accumulated energies of the material acting on the belt allows an observation that the highest values of the accumulated normal energy occur in the case of the transfer point prior to modifications, and are 1028 J. The maximum value obtained for the variant with the chute is 4-fold lower and is 265 J. The analysis of

the accumulated contact energies from tangential forces also confirms a significant decrease for the variant of the transfer point with a chute (Fig. 5 and Fig. 9).

4. Analysis of abrasive wear of the belt on the receiving conveyor

Conveyor belt wear due to its abrasion caused during the feeding of the material may be calculated with the use of normal impact energy and the slip velocity between the material and the belt, as in the relationship below [9]:

$$W_a = \mu_b \cdot \rho_{bl} \cdot V_y^2 (V_b - V_x) \left[Pa \cdot \frac{m}{s} \right] \quad (1)$$

where:

- W_a – abrasive wear of the conveyor belt $\left[Pa \cdot \frac{m}{s} \right]$,
- μ_b – coefficient of static friction between the material and the conveyor belt [-],
- V_y – normal velocity of the material at the moment of impact against the belt [m/s],
- V_x – tangential velocity of the material at the moment of impact against the belt [m/s],
- V_b – belt speed [m/s],
- ρ_{bl} – volumetric density of the material [kg/m³].

However, relationship (1) does not account for a number of factors which are important for defining belt wear at a certain point. Authors in publication [4] proposed to introduce such corrections to this equation that would allow for the inclination of the side fragments of the belt. Normal velocity of the material at the moment of impact against the belt V_y was substituted with velocity perpendicular to the belt V_{\perp} , which in the case of the inclined belt fragments is not equal to the velocity along axis Y. The second modification consisted in the introduction of the absolute value of the difference between belt velocity and material velocity parallel to the belt. This modification allowed the elimination of the negative values of belt wear in certain points selected for the analyses. Equation (1) thus transformed to be used in further calculations takes the following form:

$$W'_a = \mu_b \cdot \rho_{bl} \cdot V_{\perp}^2 |V_b - V_{\parallel}| \left[Pa \cdot \frac{m}{s} \right] \quad (2)$$

where:

Table 1. Reference conditions for relative wear

Parameter	μ_{bs} [-]	ρ_{bls} [kg/m ³]	$V_{\perp s}$ [m/s]	V_{bs} [m/s]	$V_{\parallel s}$ [m/s]	W_s [Pa·m/s]	ω_s [-]
Reference value	0.25	1000	1	2	1	250	1

V_{\perp} – material velocity normal to the belt surface [m/s],

V_{\parallel} – material velocity tangential to the belt [m/s].

The analyzed values obtained from the simulation data depend on the adopted sampling method. The simulations allow bin groups to be generated. These are virtual cubes situated over the analyzed conveyor belt. The bins record selected parameters of the material occurring in the simulation: its mean velocity or the masses of its particles. Importantly, belt wear is slower in the fragments filled with material to a lesser extent, i.e. the ones on which the material exerts a smaller force. Direct introduction of material weight into the equation would cause the calculated values of belt wear for the selected, differently sized bins to be incomparable. Therefore, standard values have been introduced (Table 1), which serve as reference for the values calculated in certain points. The proposed indicator of relative point wear (3) for each of the analyzed variants will allow the rate of abrasive wear to be determined for each point in comparison to the case in which the transported material has standard values referenced in Table 1, and the bin is completely filled with material:

$$\omega_{n,k} = \frac{\bar{F}_{\perp n,k}}{g \cdot V_{bin} \cdot \rho_{bls} \cdot \cos(\alpha)} \cdot \frac{W'_{a,n,k}}{W_s} \cdot [-] \quad (3)$$

where:

$\omega_{n,k}$ – indicator of point abrasive belt wear [-],

$\bar{F}_{\perp n,k}$ – average force acting perpendicular to the belt on each measurement bin [N],

g – gravitational constant [m/s²],

V_{bin} – volume of the bin in which the point measurement is performed [m³],

ρ_{bls} – volumetric density of the reference material [kg/m³],

α – belt inclination at a certain point [°].

If successive sampling points across the belt width are marked with the letter ‘k’, and along the belt length – with the letter ‘n’, and if the mean value of the point wear indicator is calculated for the identical n, then a relative wear indicator of the belt profile is formulated:

$$\vartheta_k = \frac{\sum_{n=1}^n \omega_{n,k}}{n} \cdot [-] \quad (4)$$

For the purpose of analyzing the abrasive belt wear, bins were added in the simulation. Their dimensions were 5x5 cm and 20 cm in height. A 10 s long simulation served to export data on mean velocity and the total mass of the particles inside the bins. The data were used to determine velocity distribution on the belt (Fig. 10). The particles which reach the belt in the variant of the transfer point with the chute clearly have a significantly higher initial velocity, and thus the zone in which they accelerate to the rated velocity is much shorter.

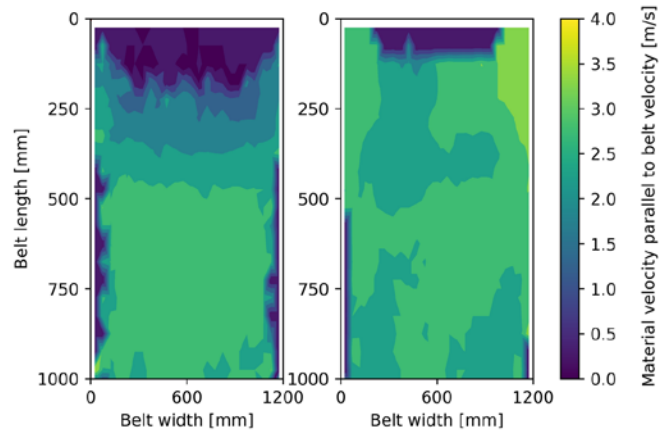


Fig. 10. Distribution of the material velocity tangential to the conveyor belt: on the left – without a chute, on the right – with a chute

The derived equations (3, 4) served to find belt areas most prone to abrasive wear (Fig. 11). The chute reduces belt wear, as it causes the lumps falling on the belt to have low normal velocity and high tangential velocity. Such a design solution allows point wear to be reduced by an order of magnitude. Provided in the graphs of Fig. 11, the belt profile wear indicators show mean values of the point wear indicator from the upper graphs, as observed along the belt width. The extremum observed in Fig. 11a was caused by the presence of larger lumps on the right side of the belt during the analyzed fragment of the simulation.

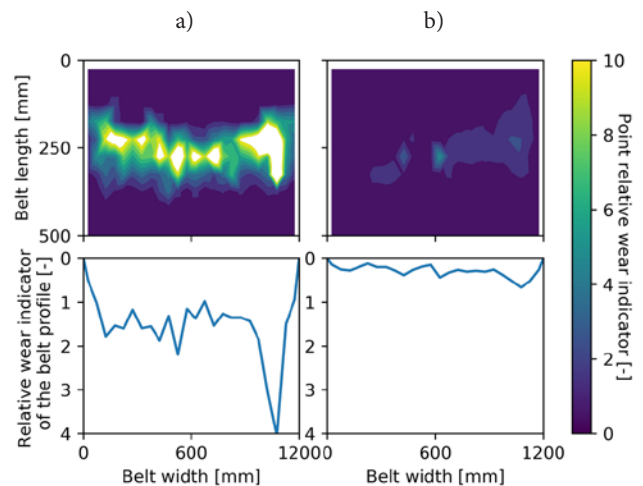


Fig. 11. Comparison of relative belt wear indicators: a) variant without chute, b) variant with chute

5. Conclusion

The article analyzes the flow of ore particles stream for a transfer point in a belt conveyor system operated in an underground copper ore mine. Discrete element method was used to identify the discharge

trajectory and to evaluate the phenomena involved in the transfer of the material onto the receiving conveyor, with particular focus on the changing values of tangential and normal velocities of the material.

In order to fully simulate the behavior of the transported material in the model, a two-stage calibration test methodology was developed. It allowed the verification of the material parameters assumed in the simulations.

In the first stage of the simulation tests, the analysis covered the current solution, in which the feeding conveyor transfers the material directly onto the belt of the receiving conveyor. The stream of material was demonstrated to have a normal velocity of approximately 6.3 m/s at the moment of collision with the receiving belt. This velocity is further reduced so that in effect the entire energy of the falling material is received by the belt. The significantly reduced tangential velocity of the material particles at the moment of contact with the belt was observed to necessitate their acceleration until the belt rated velocity was reached. This acceleration generated additional resistances to motion.

In the second stage, optimization actions were suggested with a view to improving the energy consumption of the transfer point and to reducing the negative impact of the transported material on the belt

of the receiving conveyor. The use of a modernized transfer point version with a chute resulted in a higher tangential velocity of the material particles and in a 6-fold reduction of its normal component. This solution significantly reduced the destructive influence of the material masses falling on the conveyor belt and on the feeding idler sets.

In order to identify the negative influence of the transported material on the belt of the receiving conveyor, a relative point wear indicator was proposed. Based on the results of the simulations, it allowed identifying the rate of abrasive wear individually for each of the analyzed belt fragments. The data from the simulations, read inside the bins, served to calculate the tangential velocity distribution for the material and to identify areas most prone to abrasive wear across the entire belt width. The analysis demonstrated that the use of a chute which redirects the material stream may result in as much as a 10-fold reduction of belt wear on the receiving conveyor.

Acknowledgement

The research work co-funded with the research subsidy of the Polish Ministry of Science and Higher Education granted for 2020.

References

1. E.M.A, Belt Conveyors for Bulk Materials, Conveyor Equipment Manufacturers Association, 2005.
2. Coetzee C J. Calibration of the discrete element method. *Powder Technology* 2017; 310: 104-142, <https://doi.org/10.1016/j.powtec.2017.01.015>.
3. Czuba W, Furmanik K. Analiza ruchu ziarna w przesypie przenośników taśmowych. *Transport Przemysłowy i Maszyny Robocze* 2013; 4: 12-17.
4. Doroszuk B, Król R. Analysis of conveyor belt wear caused by material acceleration in transfer stations. *Mining Science* 2019; 26: 189-201, <https://doi.org/10.37190/msc192615>.
5. Doroszuk B. *Badania Materiałowe i Modelowe Rudy Miedzi w Metodzie Elementów Dyskretnych (praca niepublikowana)*. Wrocław, 2019.
6. Doroszuk B, Walker P, Król R. Badania własności zróżnicowanej litologicznie rudy miedzi na potrzeby modelowania DEM. *CUPRUM - Czasopismo Naukowo-Techniczne Górnictwa Rud* 2019; 1: 5-19.
7. Gładysiewicz L et al. Optymalizacja rozwiązań technicznych przenośników taśmowych w PGE Bełchatów SA. Zadanie 3: Optymalizacja przesyków przenośnikowych. Raporty Inst. Gór. PWroc. Ser. SPR nr 1, 97 s. (praca niepublikowana), Wrocław, 2011.
8. Gładysiewicz L. *Przenośniki Taśmowe teoria i obliczenia*, Wrocław: Oficyna wydawnicza Politechniki Wrocławskiej, 2003.
9. Grima A, Hastie D, Fraser T, Wypych P. Discrete Element Modelling: Trouble-Shooting And Optimisation Tool For Chute Design. *BELTCON 16 International Materials Handling Conference*. Johannesburg, 2011.
10. Gutierrez A, Garate G A. Design of a Chute for Multiple Operating Conditions. *ASME International Mechanical Engineering Congress and Exposition*, 2014, <https://doi.org/10.1115/IMECE2014-36414>.
11. Hastie D, Wypych P. Experimental validation of particle flow through conveyor transfer hoods via continuum and discrete element methods. *Mechanics of Materials* 2010; 4: 383-394, <https://doi.org/10.1016/j.mechmat.2009.11.007>.
12. Hastie D. *Belt Conveyor Transfers: Quantifying and Modelling Mechanisms of Particle Flow*. Wollongong: University of Wollongong, 2010.
13. Hastie D, Grima A, Wypych P. *Modelling and Design of Complete Conveyor Transfers*. 2nd Annual Conveyors in Mining, Perth, 2008.
14. Huque S T. *Analytical and Numerical Investigation Into Belt Conveyors Transfers*, Wollongong: University of Wollongong, 2004.
15. Ilic D, McBride B, Katterfeld A. Validation of continuum methods utilizing discrete element simulations as applied to a slewing stacker transfer chute. *9th International Conference on Bulk Materials Storage, Handling and Transportation*. Newcastle, 2007.
16. Karwat B, Machnik R, Niedźwiedzki J, Nogaj M, Rubacha P, Stańczyk E. Calibration of bulk material model in Discrete Element Method on example of perlite D18-DN. *Eksploracja i Niezawodność - Maintenance and Reliability* 2019; 21 (2): 351-357, <https://doi.org/10.17531/ein.2019.2.20>.
17. Katterfeld A, Groger T, Hachmann M, Becker G. Usage of DEM simulations for the development of a new chute design in underground mining. *6th International Conference for Conveying and Handling of Particulate Solids*. Brisbane, 2009.
18. Katterfeld A. Understanding granular media: from fundamentals and simulations to industrial application. *Granular Matter* 2017; 21, <https://doi.org/10.1007/s10035-017-0765-y>.
19. Kessler F, Prenner M. DEM - Simulation of Conveyor Transfer. *FME Transactions* 2009: 185-192.
20. Korzeń Z. The Dynamics of Bulk Solids Flow on Impact Plates of Belt Conveyor Systems. *Bulk Solids Handling* 1988; 12: 689-697.
21. Mascarenhas F, Mesquita A, Mesquita A L. Simulation of transfer chute operation using the Discrete Element Method. *Cilmace* 2013. Pirenópolis, Brazil, 2013.
22. Quist J, Evertsson M. Framework for dem model calibration and validation. *Proc. of the 14th European Symposium on Comminution and Classification*, Gothenburg, Sweden, 2015.

23. Roberts A. Chute Performance and Design for Rapid Flow Conditions. *Chemical Engineering and Technology* 2003; 163-170, <https://doi.org/10.1002/ceat.200390024>.
24. Walker P, Kawalec W, Król R. Application of the Discrete Element Method (DEM) for Simulation of the Ore Flow Inside the Shaft Ore Bunker in the Underground Copper Ore Mine. *Advances in Intelligent Systems and Computing* 2019; 835: 633-644, https://doi.org/10.1007/978-3-319-97490-3_60.

Piotr WALKER

Błażej DOROSZUK

Faculty of Geoengineering, Mining and Geology
Wrocław University of Science and Technology
Wybrzeże Stanisława Wyspiańskiego 27, 50-370 Wrocław, Poland

Robert KRÓL

Department of Mining and Geodesy
Faculty of Geoengineering, Mining and Geology
Wrocław University of Science and Technology
Wybrzeże Stanisława Wyspiańskiego 27, 50-370 Wrocław, Poland

E-mail: piotr.a.walker@gmail.com, blazej.doroszuk@pwr.edu.pl,
robert.krol@pwr.edu.pl
